

Jan M. Skowroński · Mariusz Walkowiak

## Lithium intercalation into CrO<sub>3</sub>-GIC and its derivatives

Received: 15 November 2002 / Accepted: 11 June 2003 / Published online: 2 October 2003  
© Springer-Verlag 2003

**Abstract** Graphite intercalation compound with chromium trioxide (CrO<sub>3</sub>-GIC) was used as a precursor for new graphite composites. By heating CrO<sub>3</sub>-GIC at 800 °C in air a composite material, expanded graphite/Cr<sub>2</sub>O<sub>3</sub>, was obtained, whereas further heating of this composite at 1000 °C in the stream of hydrogen/argon mixture led to the reduction of Cr<sub>2</sub>O<sub>3</sub> to chromium carbide (Cr<sub>3</sub>C<sub>2</sub>). A new material thus obtained was expanded graphite/Cr<sub>3</sub>C<sub>2</sub> composite. The chromium species having catalytic properties gave rise to the improvement of the crystal structure of expanded graphite. All materials were tested as anode materials for lithium-ion cell. It was found that graphitic material treated in H<sub>2</sub>/Ag at 1000 °C has greater reversible capacity in comparison to the original graphite and the shape of the charge/discharge curve shows very well-defined stage structure which supports the crystallographic data.

**Keywords** CrO<sub>3</sub>-GIC · Expanded graphite · Graphite-based composites · Graphite anode · Lithium-ion battery

### Introduction

Exfoliation of graphite intercalation compounds creates new graphitic materials having substantially different properties compared to the original graphite. Upon

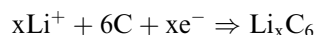
Presented at the 3rd International Meeting “Advanced Batteries and Accumulators”, June 16th–June 20th, Brno, Czech Republic

J. M. Skowroński (✉)  
Institute of Chemistry and Technical Electrochemistry, Poznań  
University of Technology, ul. Piotrowo 3, 60–965 Poznań, Poland  
E-mail: jan.skowronski@put.poznan.pl

M. Walkowiak  
Central Laboratory of Batteries and Cells, ul. Forteczna 12,  
61–362 Poznań, Poland

expansion the flake surface area increases markedly which is accompanied by a destruction of the material crystal structure. This phenomenon can be considered as a peculiar type of grinding of the graphite flakes.

In recent two decades carbons have found new important application as anodic materials for lithium-ion batteries. Although a great number of various carbonaceous materials have been tested, graphites still seem to be the best choice. The basic electrochemical process occurring during charging graphite electrode involves the reaction of lithium intercalation (lat. *intercalare* - insert, slip into) between graphene layers according to the general equation:



The maximum amount of lithium that can be reversibly intercalated into graphite host is one lithium atom per six carbon atoms, which corresponds to the electrical charge 372 mA per gram of graphite. The reversible capacity ( $Q_{\text{rev}}$ ) can be described as the accessible capacity of the electrode gained on discharging performed after the first charging. A certain fraction of electrical charge delivered to the graphite electrode during the first charging cannot be regained upon the subsequent discharging. The difference between the electrical charge put in the electrode during the first charging ( $Q_{1\text{ch}}$ ) and that recovered during the first discharging ( $Q_{1\text{dis}}$ ) is called the irreversible capacity ( $Q_{\text{irr}}$ ). The term *efficiency* also used in technical literature is defined as the ratio  $Q_{1\text{dis}}/Q_{1\text{ch}}$ , often expressed in percents. The value of  $Q_{\text{irr}}$  results mostly from the electrolyte decomposition leading to the formation of so-called solid electrolyte interface (SEI). Excessively high value of  $Q_{\text{irr}}$  is undesirable since it lowers the battery energy density.

It was shown that exfoliated graphite provides larger reversible capacity of lithium intercalation compared to the original graphite [1, 2]. It was also proved that mechanical grinding of graphite flakes has a strong influence on both the reversible and irreversible

capacities [3, 4, 5]. Both phenomena can be explained in terms of facilitated transport of lithium ions within the graphite structure. Unfortunately, also the irreversible capacity may rise after exfoliation due to the increase in surface area.

In an earlier work [6] we examined the chemical composition and structure properties of some graphite-based materials obtained by thermal exfoliation of  $\text{CrO}_3$ -GIC. This compound was exfoliated in air at 800 °C, and the material obtained this way was subsequently heat-treated at 1000 °C in the flow of hydrogen. The present paper aims at analysing the lithium insertion/de-insertion behaviour of a wide range of materials derived from  $\text{CrO}_3$ -GIC.

## Experimental

Stage-6  $\text{CrO}_3$ -graphite intercalation compound ( $\text{CrO}_3$ -GIC) was synthesized by the so-called solvent method described in [7] using natural flaky graphite (99.9 wt.% C, flakes in the diameter range 180–200  $\mu\text{m}$ ) donated by Graphitwerk Kropfmühl AG, Germany. X-ray diffraction (XRD) analysis showed that stage-6  $\text{CrO}_3$ -GIC (c-axis repeat distance  $L_c = 2.4930$  nm) is admixed with the phase of pure graphite. The C/Cr ratio of 32.3 was estimated by chemical analysis. Thermal exfoliation of  $\text{CrO}_3$ -GIC was carried out by placing a ceramic vessel containing the GIC sample for 10 min in a laboratory oven heated to appropriate temperature (800 °C). Samples subjected to hydrogen treatment were heated slowly in a quartz tube using a pipe oven until the desired temperature was reached (1000 °C) and then kept in this temperature for a given period of time. The XRD measurements were carried out using X-ray diffractometer (Phillips PW-1710, 35 kV, 20 mA) with  $\text{FeK}\alpha$  radiation ( $\lambda = 0.1937$  nm). The lithium insertion/de-insertion behaviour of samples were examined in a two electrode coin cell (CR 2430-type) with a lithium foil playing simultaneously role of both the counter and reference electrode. The electrolyte was 1 M  $\text{LiClO}_4$ -EC/DEC (1:1 by weight). The working electrodes were prepared by mixing the sample (80 wt.%) with acetylene black (10 wt.%) and PVDF (10 wt.%) dissolved in cyclopentanone. After spreading the slurry on the nickel grid current collector the electrodes were dried under vacuum at 140 °C for 4 h. The cells mounted in the glove box filled with dry argon were galvanostatically cycled between 0 V and 2 V vs.  $\text{Li}/\text{Li}^+$  at a rate of 10 mA/g of active substance. The potential curves plotted from 2 V to 0 V correspond to the charge run of electrode.

## Results and discussion

Table 1 shows the sequence of experimental procedures starting from natural graphite (denoted GK180), which was subsequently intercalated with chromium trioxide

(sample  $\text{CrO}_3$ -GIC). The resulting graphite intercalation compound is stage-6 compound which means that two neighbouring layers of intercalate ( $\text{CrO}_3$ ) are separated by six graphene layers.  $\text{CrO}_3$ -GIC exhibits the so-called ash-tray distribution of intercalate within the graphite flake. For such a case intercalate is located preferably in the edge regions of the graphite flakes. Figure 1 shows the galvanostatic charge/discharge curves for the starting graphite and  $\text{CrO}_3$ -GIC. As compared to the graphite precursor (Fig. 1a),  $\text{CrO}_3$ -GIC (Fig. 1b) is characterised by a significantly smaller reversible (discharge) capacity (see Table 1), which can easily be explained by the fact that some interlayer spacings of graphite in  $\text{CrO}_3$ -GIC are occupied by the primary intercalate,  $\text{CrO}_3$ . Another striking feature in Fig. 1b is a huge irreversible capacity. Such a large retention of charge cannot be attributed only to the formation of the

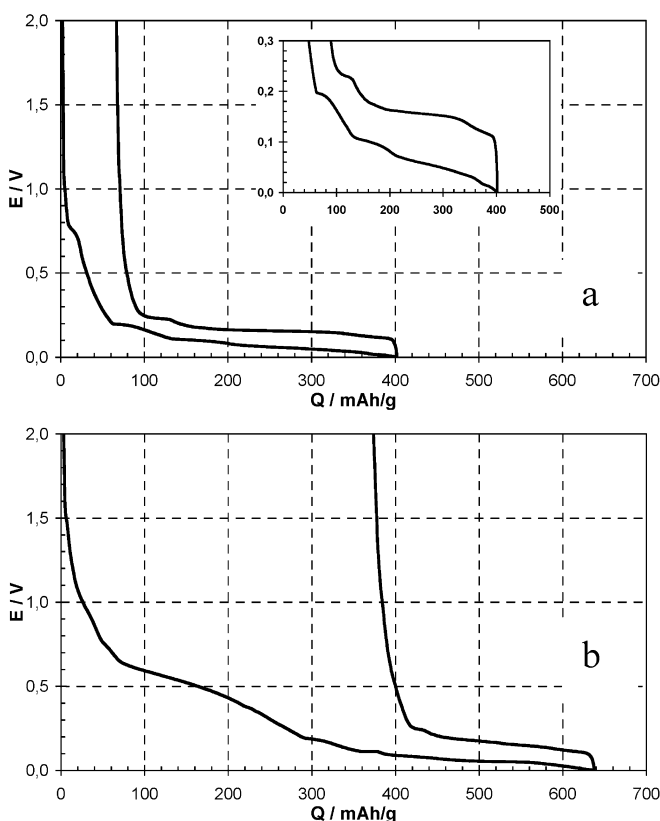


**Fig. 1a, b** Galvanostatic charge/discharge curves for sample GK180 with enlarged potential region 0–0.3 V (a) and for sample  $\text{CrO}_3$ -GIC (b)

**Table 1**

Sample	Description	$Q_{1\text{ch}}$ (mAh/g)	$Q_{1\text{dis}}$ (mAh/g)	Efficiency (%)	$d_{002}$ (nm)	$L_c$ (nm)
GK180	Natural graphite	400	322	81	0.3356	336
$\text{CrO}_3$ -GIC	Graphite GK180 intercalated with $\text{CrO}_3$	635	263	41	0.3352	-
CR800	$\text{CrO}_3$ -GIC exfoliated at 800 °C in air	709	446	63	0.3366	60
CR800/H1000	CR800 after treatment in $\text{H}_2$ at 1000 °C	469	185	39	0.3352	222
CR800/H1000/ G1/HCL	CR800/H1000 after removal of $\text{Cr}_3\text{C}_2$	442	354	80	0.3352	237

solid electrolyte interface (SEI) at the flakes surface, but also to lithium ion co-intercalation into the graphite galleries where  $\text{CrO}_3$  is accommodated. There is no indication of electrochemical reduction of  $\text{CrO}_3$  between the graphene layers, which is in agreement with earlier report [8].

Thermal treatment of  $\text{CrO}_3$ -GIC at 800 °C brings about the violent decomposition of intercalate with the accompanying evolution of  $\text{O}_2$  and  $\text{CO}_2$ . The product of this reaction is lower chromium oxide,  $\text{Cr}_2\text{O}_3$  (for crystallographic evidence see Fig. 2), which is ejected outside the graphite galleries.  $\text{Cr}_2\text{O}_3$  thus obtained forms a composite material together with the expanded graphite created during the thermal shock (sample CR800). Exfoliation gives rise to the worsening of structural perfection of graphite. As a consequence, a significant diminishing of the average crystallite dimensions along c-axis ( $L_c$ ) is noted for expanded graphite (compare samples GK180 and CR800 in Table 1). Electrochemical test for sample CR800 (Fig. 3) shows that lithium is intercalated independently into graphite and  $\text{Cr}_2\text{O}_3$ . The sloping part (above ca. 0.2 V) on the discharge curve can be attributed to de-insertion of lithium ions from  $\text{Cr}_2\text{O}_3$ , whereas the rest of this curve (below ca. 0.2 V) has a shape typical for de-intercalation of lithium ions from graphite lattice. In the case of  $\text{Cr}_2\text{O}_3$  the term *insertion* should be used rather instead of *intercalation*, since the

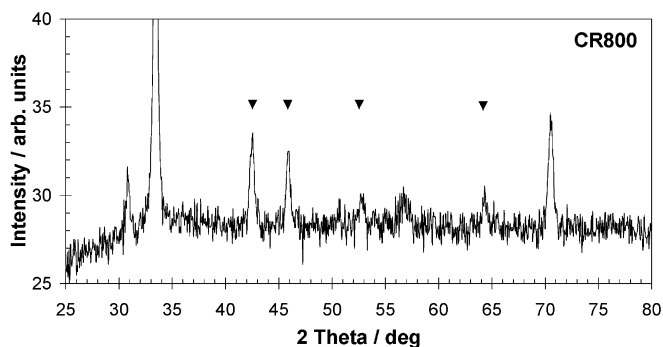


Fig. 2 XRD pattern for sample CR800 with marked reflections for  $\text{Cr}_2\text{O}_3$

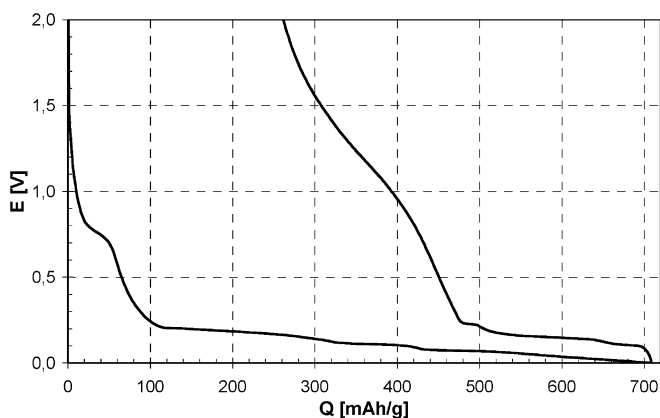


Fig. 3 Galvanostatic charge/discharge curves for sample CR800

latter is appropriate to the reaction proceeding in layered structures.

After heat-treatment of sample CR800 in the flow of hydrogen and argon,  $\text{Cr}_2\text{O}_3$  disappears on the expanded graphite particles owing to the creation of a new phase of chromium carbide,  $\text{Cr}_3\text{C}_2$  (Fig. 4). The product of this reaction is denoted CR800/H1000. A very striking phenomenon occurring for this sample is an improvement of the structural ordering of graphite. As can be seen in Table 1, the crystallite size rose from 60 nm for the material before heat-treatment by hydrogen (sample CR800) to 222 nm after this treatment (sample CR800/H1000). This phenomenon is so interesting for two reasons. The first one is that the re-graphitisation process takes place in the temperature as low as 1000 °C, whereas normally the graphitisation process requires temperatures close to 3000 °C. The second reason is that the phenomenon concerns exfoliated graphite. The possibility of rebuilding the destroyed structure of expanded graphite has never been reported so far. We attribute the restoration of the structural perfection to the catalytic action of chromium species. It is open question as to the chemical nature of chromium species catalysing the re-graphitisation of expanded graphite. According to the mechanism of the  $\text{Cr}_3\text{C}_2$  formation proposed in our previous work [6], the possible intermediate step in this process is the formation of very dispersed metallic chromium particles playing the role of the graphitisation catalyst, like other transition metals (e.g., Fe, Ni). Unfortunately, it was impossible to detect chromium in sample CR800/H1000 by means of techniques used in this work. Besides even if metallic chromium appears during the process of heat-treatment in hydrogen, it probably disappears instantly in the reaction with graphite to give chromium carbide. Taking this into account, it seems more justified to assign the catalytic function to chromium carbide.

The presence of  $\text{Cr}_3\text{C}_2$  greatly affects the electrochemical behaviour of the composite material. Since this compound is not capable of hosting lithium ions it can be considered as a kind of inactive ballast which increases the electrode weight, and in turn, contributes to the decrease in the electrode capacity. The charge/discharge curves for sample CR800/H1000 in Fig. 5 show a

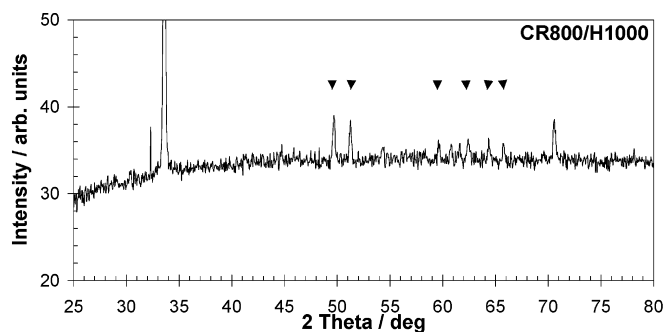
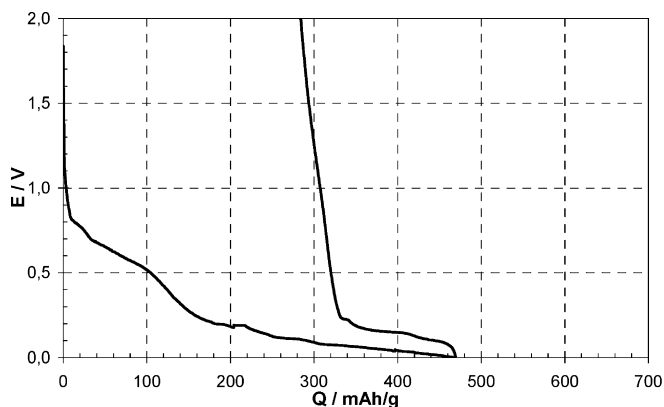
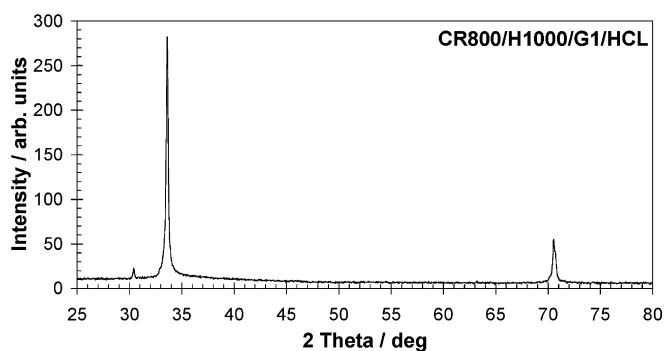


Fig. 4 XRD pattern for sample CR800/H1000 with marked reflections for  $\text{Cr}_3\text{C}_2$



**Fig. 5** Galvanostatic charge/discharge curves for sample CR800/H1000



**Fig. 6** XRD pattern for sample CR800/H1000/G1/HCL

low reversible (discharge) capacity as well as a low efficiency (see also data for sample CR800/H1000 in Table 1).

The presence of chromium carbide makes the comprehensive assessment of the electrochemical behaviour of the restored expanded graphite difficult. The phase of  $\text{Cr}_3\text{C}_2$  strongly influences the shape of the galvanostatic curves as well as the XRD pattern. Due to the presence of  $\text{Cr}_3\text{C}_2$  some properties of the graphite component are masked to some extent. For this reason, in the last step on the preparation way the carbide component was removed from sample CR800/H1000 by treating it in boiling alkaline solution of  $\text{KMnO}_4$  followed by washing in dilute HCl. As is proven by the XRD pattern (Fig. 6), the material thus obtained (labelled CR800/H1000/G1/HCL) is pure graphite. Figure 7 shows the respective charge/discharge curves for chemically purified sample. The character of these curves corresponds to well ordered structure (defined stages of intercalation are represented by the potential plateaux), which is in accordance with crystallographic data (Table 1). The reversible capacity of this electrode ( $Q_{\text{dis}} = 354 \text{ mAh/g}$ , see Table 1) is close to the theoretical capacity for graphite and is ca. 10% higher than that of the starting graphite (sample GK180). At the same time, the efficiency in the first cycle remained at

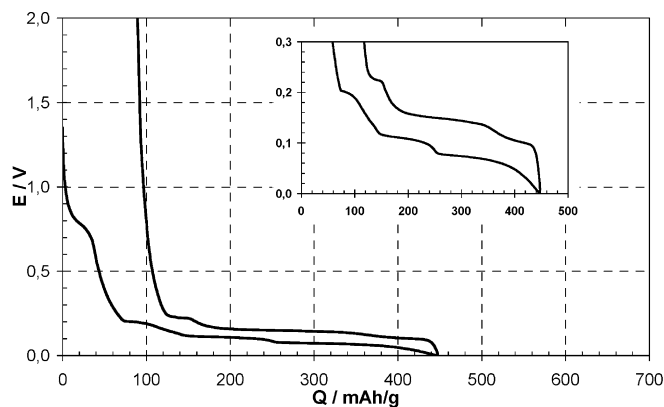


**Fig 7** Galvanostatic charge/discharge curves for sample CR800/H1000/G1/HCL with enlarged potential region 0–0.3 V

the same level (80% as compared to 81% for sample GK180, see Table 1). The enhanced reversible capacity for graphite CR800/H1000/G1/HCL can be related to the changes in structure occurring during the catalytic reaction. Owing to the formation of well stacked graphene layers (larger crystallites), graphite electrode can host the maximum amount of lithium ions (capacity corresponding nearly to  $\text{LiC}_6$ ). Smaller hysteresis (the potential difference between charge and discharge curves) on the plot for new graphite (compare Fig. 1a and 7) can be explained in terms of facilitated transport of lithium ions in the bulk of the electrode. It is very likely that thermal exfoliation of graphite opened new paths for fast ionic transport in the crystal structure.

## Conclusions

Upon heat-treatment at 1000 °C in hydrogen the composite graphite- $\text{Cr}_2\text{O}_3$  (obtained by thermal exfoliation of  $\text{CrO}_3$ -GIC) changes to another composite graphite- $\text{Cr}_3\text{C}_2$ . The side effect of this transformation is the restoration of the graphite structure, which was previously destroyed due to exfoliation. The present paper gives a strong electrochemical evidence for this structural restoration. The new graphite can reversibly accommodate ca. 10% lithium more than the original graphite, and the shape of the charge/discharge curves reveals a very well-defined stage structure.

**Acknowledgements** This work was partially supported from the State Committee for Scientific Research of Poland (KBN Grant No. 3 T09B 068 19).

## References

1. Fukuda K, Kikuya K, Isono K, Yoshio M (1997) *J Power Sources* 69:165
2. Skowroński JM, Walkowiak M (2000) *Mol Phys Reports* 27:103
3. Disma F, Aymard L, Dupont L, Tarascon J-M (1996) *J Electrochem Soc* 143:3959

4. Winter M, Novak P, Monnier A (1998) *J Electrochem Soc* 145:428
5. Wang H, Ikeda T, Fukuda K, Yoshio M (1999) *J Power Sources* 83:141
6. Skowroński JM, Walkowiak M (2001) *Karbo* 11:400
7. Skowroński JM (1996) *J Phys Chem Solids* 57:695
8. Besenhard JO, Schollhorn R (1977) *J Electrochem Soc* 124:968